INPE-11287-PRE/6724

PARTICLES'S RELATIVE VELOCITIES ON DIFFERENT ORBITAL RATIOS ACROSS CIRCULAR ORBITS SUBJECT TO THE RADIATION PRESSURE

Cláudia C. Celestino*
Othon C. Winter
Antonio Fernando Bertachini de Almeida Prado

PARTICLES'S RELATIVE VELOCITIES ON DIFFERENT ORBITAL RATIOS ACROSS CIRCULAR ORBITS SUBJECT TO THE RADIATION PRESSURE

C. C. Celestino*
O. C. Winter , **A. F.B.A. Prado**

*Divisão de Mecânica Espacial e Controle, Instituto Nacional de Pesquisas Espaciais,
INPE, 12227-010 São José dos Campos, SP, Brasil.
E-mail: claudia@feg.unesp.br*

ABSTRACT

In the present work we consider a dynamical system of μm size particles around the Earth subject to the effects of radiation pressure. Our main goal is to study the evolution of its velocity relative to the circular orbits that it crosses. The initial conditions considered are the particle is in circular orbit with three semi-major axis: $a_o = 42,164$ km - geostationary orbit, $a_0 = 25,000$ km - intermediate orbit, $a_0 = 8,000$ km – low orbit. Particles size were considered in the range between 100 to 1 μm and its density is $\rho = 3$ g/cm^3. The effect of the radiation pressure produces variations in its eccentricity, resulting in a change of its orbital velocity. The results indicated that the linear momentum and kinetic energy increases as the particle size increases. For a particle of 1 μm in circular geostationary orbit the kinetic energy is initially approximately 1.56 x 10^{-7} *J* and the momentum is 6.27 x 10^{11} kg m/s and for 100 μm the energy is approximately 1.82 x 10^4 J and the momentum is 2.14 x l0^6 kg m/s.

INTRODUCTION

Circumplanetary particles are affected by a large array of perturbation forces whose relative strengths vary significantly from one situation to another. In this way, a single perturbation can dominate over all the others. When we consider objects of sizes around *μm* the orbital evolution of these small dust particles in the solar system is strongly affected by the radiation pressure force. The importance of studying the dynamics of these particles is that they can have relative high speeds and their effects in a collision could cause damages and even compromise a space mission. Many studies were made using the analytical and numerical approach to explain the dynamics of small particles around planets or the Sun under the influence of this force. Following, we introduced some of these works: Burns et al. (1979) found out an analytical expression for the radiation pressure and Poynting-Robertson drag forces for small spherical particles composed of real materials that are irradiated by the actual solar spectrum. However, their studies considered only zero inclinations and eccentricity. Mignard (1982) analytically investigated the dynamics of small particle orbiting a planet when solar radiation pressure and Poynting-Robertson drag forces are added to the planet's gravitational central field. He derived a set of differential equations in a reference frame linked to the solar motion. The case of inclined orbits is studied through a numerical integration. We can still report several works used to explain a specific

dynamical system, for example, considering the heliocentric system, in 1985, Grün et al. presented a new model of the lunar and interplanetary fluxes using *in situ* data. This new models reevaluated the size of heliocentric distribution of interplanetary meteoroids on the basis *in situ* data and analyze the probable nature of the sinks and sources of meteoritic material. They adopted a simplified mathematical model for collisional fragmentation between interplanetary objects. They showed that small particles ($m \leq 10^{-10}$ g), are most efficiently removed by radiation pressure. Hamilton and Burns (1992) determined that radiation pressure is the most efficient mechanism to remove relatively small particles of the circumasteroidal region. They showed that radiation pressure acting in a particle can cause large oscillations in the orbital eccentricity of this particle which can be driven to escape of the solar system or to collide with the asteroids. Krivov et al. (1998) model the dynamics and physical evolution of dust grains at several solar radii from the Sun. They take into account solar gravity, direct solar radiation pressure, Poynting-Robertson force, sublimation, and the Lorentz force. They suggest that the decrease of grains' sizes and the dynamics of particles in the orbital plane are well described by taking into account solar gravity and radiate forces together with the sublimation process, being relatively insensitive to the electromagnetic force. Now, if we consider circumplanetary particles, Foryta and Sicardy (1996) developed general techniques that are used to study the dynamics of Neptune's ring arcs, near the 13:12 mean motion resonances with the satellite Galatea considering effects of the radiation pressure, Poynting-Robertson drag and collisions. They showed that the pressure of solar radiation sweeps out from the arcs the particles with a ratio β of radiation pressure to solar gravitation larger than about 0.01, corresponding to 50.0 μm sized icy particles in the limit of geometrical optics. Liou and Zook (1997) develop simple analytical expressions that describe the orbital evolution of a dust grain in mean motion resonances with planets. They considered that particles are affected by solar radiation pressure, Poynting-Robertson drag and solar wind drag. The dynamical system adopted was the restricted three-body system. Ishimoto (1996) suggested the explanation for formation of the rings' dust of Phobos and Deimos. These rings are formed by small particles ejected from the Martian satellites. They show that the combination among the dynamic effect caused by Mars's oblateness and the radiation pressure plays an important role in the formation of dust rings around Mars.

In this work we are numerically studying the dynamics of particles of the order of *μm* originary from space debris around the Earth subject to the disturbances due to radiation pressure force. Our main goal is to study the evolution of its velocity relative to the circular orbits that it crosses. The initial conditions considered are the particle is in circular orbit in three different orbital regions: *a_o = 42,164* km - geostationary orbit, *a_0 = 25,000* km - intermediate orbit, *a_0 = 8,000* km – low orbit. Particles size are considered in the range between 100 to 1 μm and its density is ρ = 3 g/cm³.

DYNAMICAL SYSTEM

Small particles, μm size particles, around the Earth are subject to the effects of radiation pressure besides the gravitational force. This disturbance causes variations in the orbital evolution of these particles. The effect of the radiation pressure produces variations in its eccentricity, resulting in a change in its orbital velocity. Therefore, in this work we study the evolution of the velocity relative and the eccentricity of these particles across circular orbits of satellites around of the Earth. The illustration of the positions of hypothetical satellites in circular orbits around the Earth and a particle crossing the orbits of these satellites is presented in figure 1.
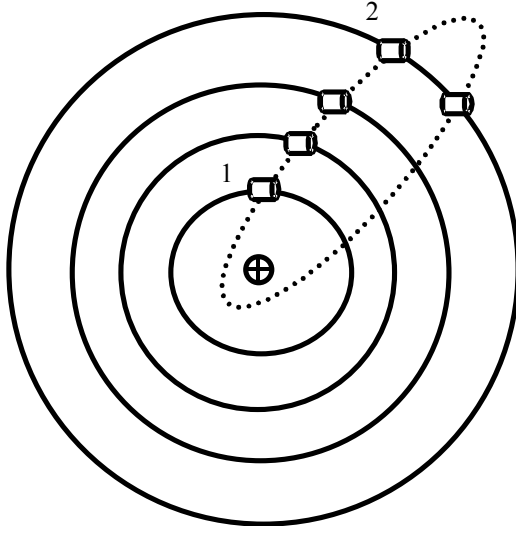
Diagram of hypothetical artificial satellites in circular orbits around the Earth (full line) and a particle in an elliptical orbit crossing the orbits of these satellites (dotted line). These satellites could be in a LEO (Low Earth Orbit, labelled 1), GEO (Geostationary Earth Orbit, labelled 2) or another orbits.

The radiation pressure force components in the planetocentric frame are given by:

$$F_x = -\frac{SA}{c} Q_{pr} \, cos(n_{Sun} t) \qquad (1)$$

$$F_y = -\frac{SA}{c} Q_{pr} \, sin(n_{Sun} t) \qquad (2)$$

where S is the solar flux, A is the particles cross section, c is the speed of light, Q_{pr} is the radiation pressure coefficient and n_{Sun} is the mean motion of the Sun around the Earth. The constant term of the above equations can be given by:

$$\frac{SAQ_{pr}}{c} = \beta F_{grSun} \qquad (3)$$

where F_{grSun} is the Sun gravitational force and β is a parameter that depends on the density of the particle and size (Burns et al., 1979).

NUMERIC SIMULATIONS

Geostationary orbit

The numerical simulation of the particle's orbital evolution, relative velocity, eccentricity and semimajor axis around the Earth is presented in this section.

The simulation of the orbital evolution of a 6 μm particle is shown in figures 2. This particle is subject to radiation pressure force and its semi-major axis is 42,164 km (geostationary particle). The thick line represents the orbit of this particle without radiation pressure. From figure 2 we note a short period effect on the orbital evolution of the particle producing large radial oscillations. Since the Sun is

initially on the negative side of the x axis and integration period was only one year the evolution of the orbit becomes asymmetric, being shifted to the direction opposite of the Sun's location.
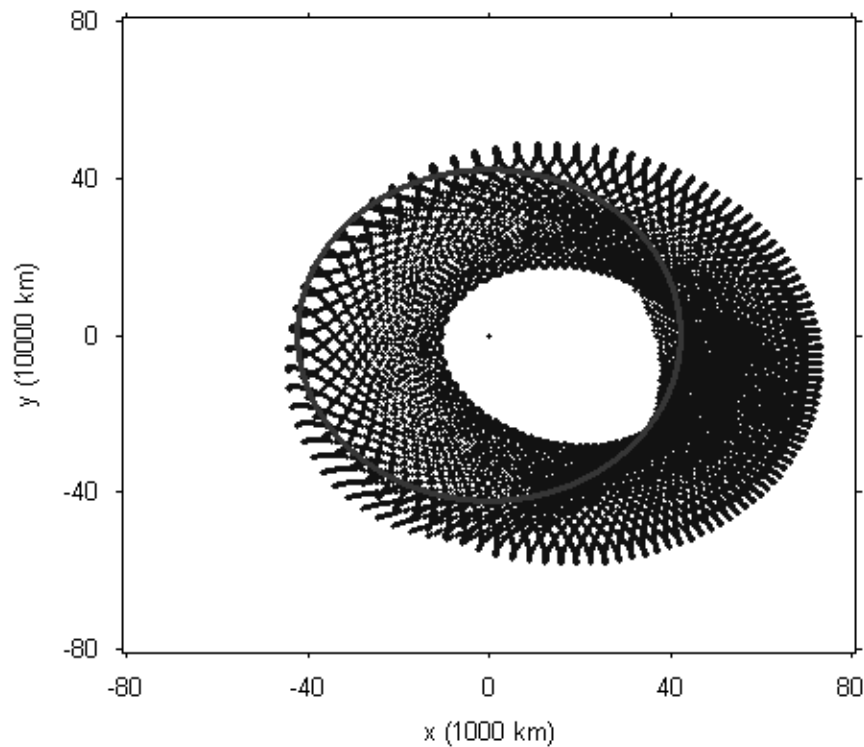

Figure 2. Orbital evolution of a 6 μm particle considering the effect of radiation pressure. The particle has initial semimajor axis of 42,164 km (geostationary orbit). The darkest line represents the orbit of this particle without radiation pressure. The radiation pressure produces an oscillatory effect on particle's unperturbed orbit. This is represented by the thin line. Note a short period effect (we considered short period the effect that happens along a particle's orbital period) on the orbital evolution of the particle producing large radial oscillations. This large radial oscillation are due to the rapidly increasing eccentricity. Since the Sun is initially on the negative side of the x axis and the integration period was only one year, the evolution of the orbit becomes asymmetric, being shifted to the direction opposite of the Sun's location.

In figures 3 and 4 is shown the evolution of the orbital radius, relative velocity, orbital evolution and eccentricity for a particle of 3 μm and 100 μm, respectively. The amplitude of radial oscillation produced on the 3 μm particle is so high that it gets too close to the Earth, where it will be removed by atmospheric drag (not considered in the present work). That happens in a time scale of less than 70 days. In the case of the 100 μm particle (figure 4) the amplitude of radial oscillation is very small. We followed the particle's evolution for several years and it repeats itself.

The variation of the eccentricity (and orbital radius) is periodic, with a long period component. If the radiation pressure is not too strong, i.e., relatively large particles, this long period is about the same as the Earth's orbital period. As the radiation pressure increases, it means small particles, the period gets smaller than that. This agrees with the results presented in Hamilton and Krivov, 1996; Krivov et al., 1996 and Juhász and Horányi, 1995. Our simulations show that the decreases in such period happens for particle size smaller then 20 μm.
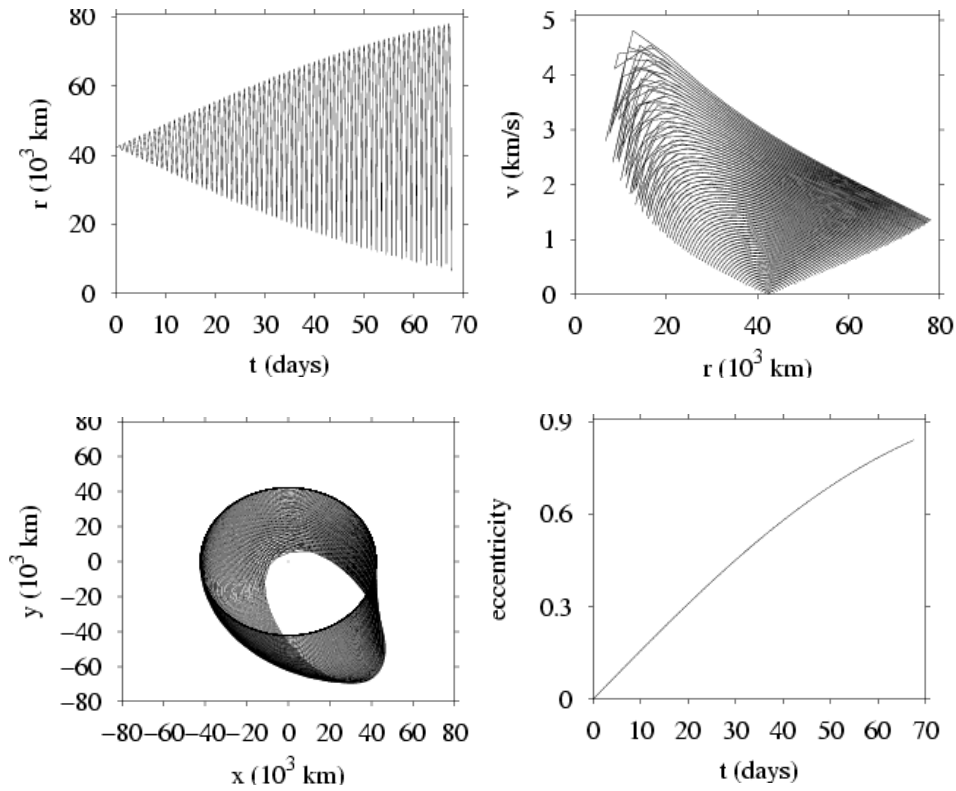
Figure 3. Evolution of the orbital radius, relative velocity, orbital evolution and eccentricity for a particle of 3 μm.

The evolution of the relative velocity (with respect to the circular orbits that the particle crosses) gives an idea of the range of possible values (intensities) as a function of radial position of target satellites. A 1 μm particle can reach a relative velocity of almost 5 *km/s* on the region of low Earth orbits, and almost 3 *km/s* on the region of geostationary orbits (where the particle was originated). Since the 100 μm particle was not removed, it shows the symmetric distribution of the relative velocity as a function of radial position. The maximum relative velocity occurs when it crosses its own initial orbit at about 0.17 *km/s*. Smaller particles present larger velocities than larger particles. These results suggest that smaller particles could offer larger risks to the target satellites than larger particles. However, when we made calculations of the kinetic energy and the linear momentum of these particles we verified that this is not the case. Larger particles present larger kinetic energy and linear momentum than smaller particles (see figures 5a and 5b). This change happens because the particle's mass is a function of r_p^3 (r_p is the particle's radius). Therefore, large particles possess large kinetic energy and linear momentum, offering higher damage. On the other hand, large particles oscillates in a very narrow ring of orbital radius, while smaller particles cover a much wider region. In figures 5a and 5b is shown the evolution of the maximum kinetic energy and linear momentum from particles from 1 to 100 μm. A fit of the points on these figures clearly indicates a bimodal behaviour. Note that particles ≤ 5 μm present linear evolution and larger particles present nonlinear evolution to time kinetic energy and linear momentum. The energy and the momentum increases as the particle size increases. For a particle of

1μm the energy is approximately 1.56 x 10^{-7} *J* and the momentum is 6.27 x 10^{-11} *kg m/s* and for 100 μm the energy is approximately 1.82 x 10^{-4} *J* and the momentum is 2.14 x 10^{-6} *kg m/s.*
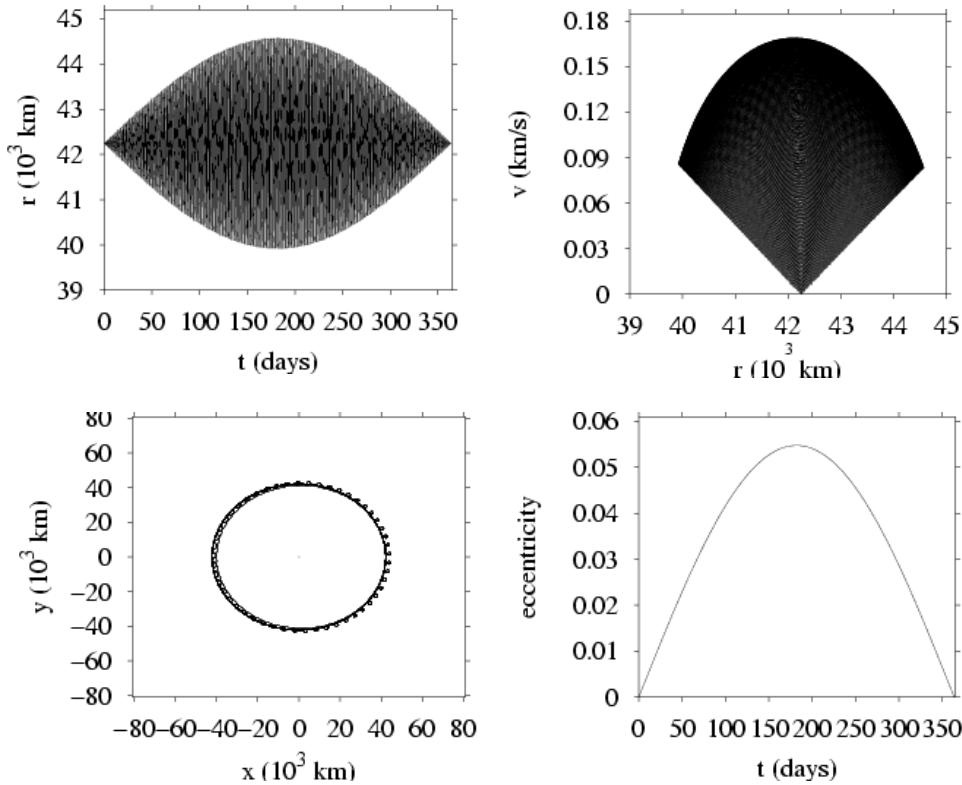
Figure 4. Evolution of the orbital radius, relative velocity, orbital evolution and eccentricity for a particle of 100 μm.

Other orbital regions

As it can be observed in the previous section, the eccentricity and the velocity and, consequently, the kinetic energy and linear momentum present different values for different particle sizes. However, the considered orbital region was geoestationary, in the exploration region around of the Earth is composed by the high, average and low regions. This way, in this section the relative velocities and the eccentricities are presented for particles from 1 to 100 μm in orbital regions of high orbits - 42,164 km, intermediate orbits - 25,000 km and lower orbits - 8,000 km

In the figure 6 the value of the maximum eccentricity is presented for particles from 1 to 100 μm for the three initial orbital ratios. It can be observed that the size of the particle and the orbital region produce different maximum values in the eccentricity variation. In high orbital region, the particle has the eccentricity maximum value of *e* ~ 0.9 and, in the intermediate orbital region, the eccentricity maximum value is *e* ~ 0.7. These values are approximately constant for sizes of particles < 6 mμ. In the lower orbital region around the Earth, particles present eccentricity maximum values of approximately 0.1 and the range of particles with this eccentricity is ≤ 20 μm.
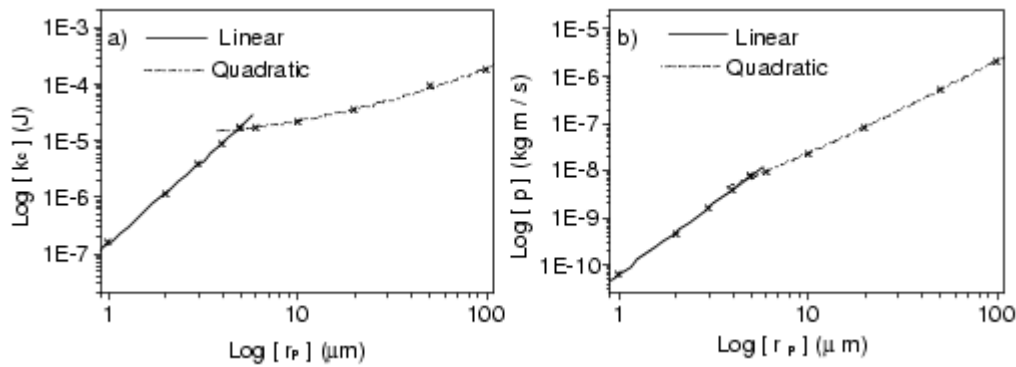
Fig. 5. a) Maximum kinetic energy for particles from 1 to 100 μm. The energy increases as the particle size increases. For a particle of 1 μm the energy is approximately 1.56×10^{-7} J and for 100 μm it is approximately 1.82×10^{-4} J and b) Maximum linear momentum for particles from 1 to 100 μm. The momentum increases as the particle size increases. For a particle of 1 μm the momentum is approximately 6.27×10^{-11} kg m/s and for 100 μm it is approximately 2.14×10^{-6} kg m/s.
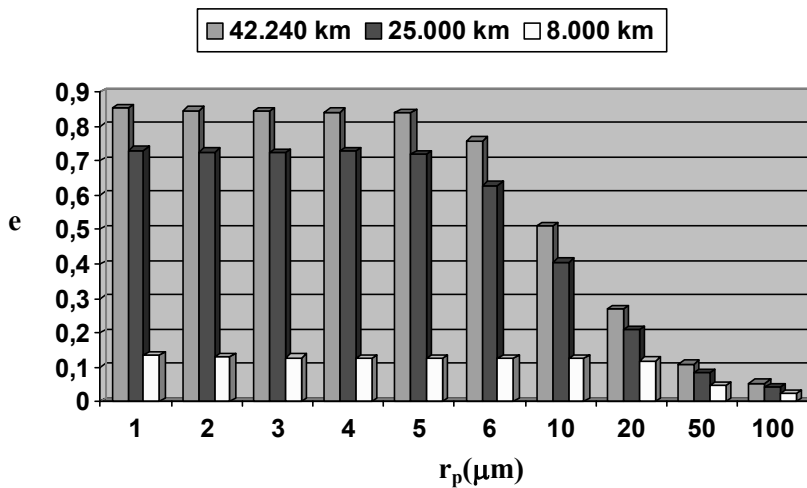

Figure 6. Maximum eccentricity versus particle size at high, intermediate and lower initial orbits around of the Earth.

The value of the maximum velocity as a function of the orbital region and of the particle size is presented in figure 7. The maximum velocity behavior presented a fact that deserves attention. It can be observed that for particles ≥ 20 μm the particle maximum velocity practically does not depend on the initial orbital region. Then, above this limit value, the radiation pressure causes the same independent effect of the particle orbital region and below this value the effect of the radiation pressure presents dependence with the size and with the particle orbital region.

Figures 8a and 8b showed the kinetic energy and linear momentum values only for particles ≤ 10 μm, because for larger particles than this value the kinetic energy and linear momentum are almost independent of the orbital region where the particle is found. In this figure, the scale used for the kinetic energy and for the linear momentum was logarithmic in order to visualize better their behavior. It is observed, that, if the particle size is fixed, the high and intermediate orbital regions around the Earth present, approximately, the same intensity of kinetic energy and of linear momentum. These

values differ in comparison with the low orbital region. Then, the radiation pressure has approximately the same effect for the same particle size in the range from 1 to 10 μm for high and intermediate orbital region of the Earth.

The amplitude of oscillation of the eccentricity and of the orbital ratio make the particle to enter in the region where the predominant disturbing force is the atmospheric drag with periods of different integration in agreement with the particle size and its orbital region. When the particle enters in this region altitude, ≤ 1,000 km, the numeric integration is interrupted because, for instance, this disturbance was neglected. Figure 9 presents the integration maximum time for the particle to enter in this region, where the predominant perturbation is the atmospheric drag in function of the particle size and its orbital area. Only in the region of intermediate orbits around the Earth particles ≥ 5 μm do not enter in the region of atmospheric drag.
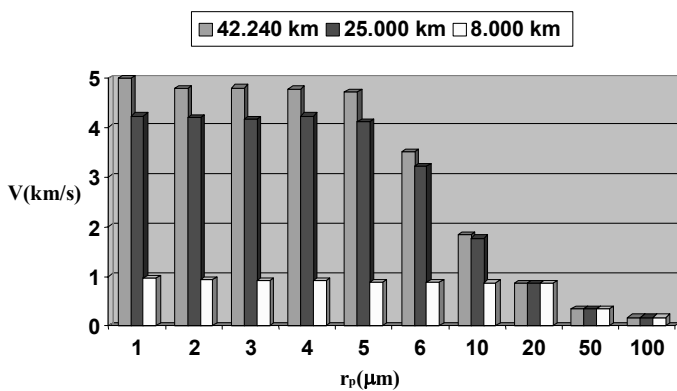

Figure 7. Maximum velocity versus particle in high, intermediate and lower orbits around of the Earth.

FINAL COMMENTS

The radiation pressure have predominant effect in particles < 5 μm. For these particle sizes time radiation pressure can be considered a natural mechanism of removal, because it causes a very large amplitude of oscillation in the eccentricity. A few days is enough for these particles to enter in the area where the predominant disturbance is the atmospheric drag. The maximum values found for the relative velocity as a function of the particle radius were: r_p = 1 μm, v = 4.99 km/s and r_p =100 μm, v= 0.17 km/s. In spite of the particles larger than 6.0 μm present smaller relative velocity, the particles momentum grow significantly, r_p =1 μm, p = 6.27 x 10^{-11} g km/s and r_p =100 μm, p = 2.14 x 10^{-6} g km/s. Therefore large particles possess large momentum, offering collision risk in spite of its orbital area be very defined. It was also seen that the radiation pressure produces an effect of short period in the eccentricity, in the orbital radius, in the semimajor axis and in the relative velocity.

Comparing the results of the numeric simulations for the case of particles in high, intermediate and low region of the Earth it verifies that the relative velocity presents similar values for particles ≥ 20 μm independently of the orbital ratio. The eccentricity variation is similar for any orbital ratio. The time for the particle to enter in the region where the predominant disturbing force is the drag depends on the size and of the orbital ratio on the particle. Particles ≥ 5 μm do not present variation in the large eccentricity to put them in the region of atmospheric drag considering the initial intermediate orbital

region, that is, $a_0 = 25,000$ km. In the high and low orbital regions particles ≤ 5 µm present eccentricity variation capable to put them in the drag region.
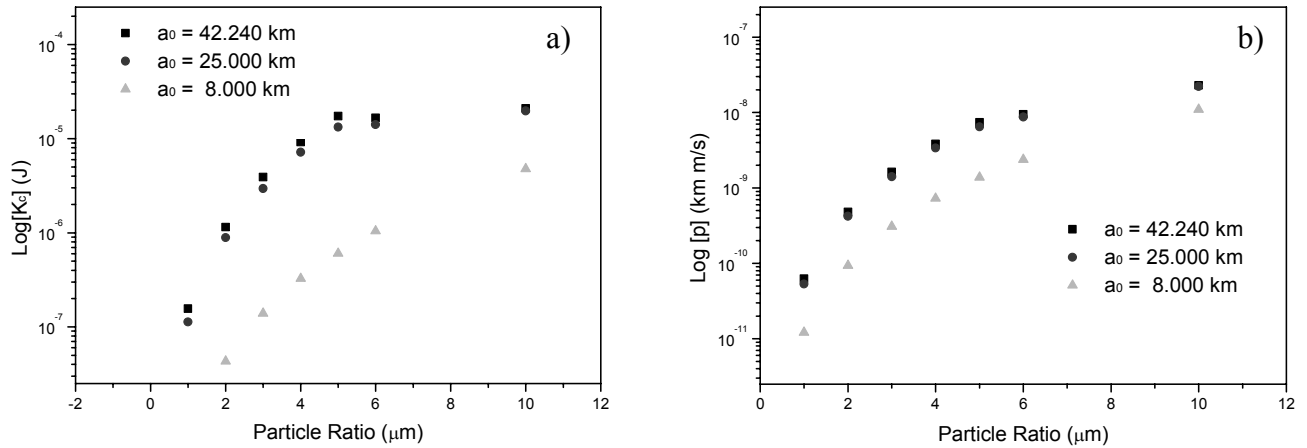

Figure 8. a) kinetic energy and b) linear momentum variation for particles ≤ 10 µm. It is observed that particles in the high and intermediate orbital regions around the Earth present, approximately, the same intensity of kinetic energy and linear momentum. These values differ when it is considered the low orbital region. Then, the radiation pressure has the same effect approximately for the same particle size in the range from 1 to 10 µm and that are in the high and intermediate orbital region of the Earth.
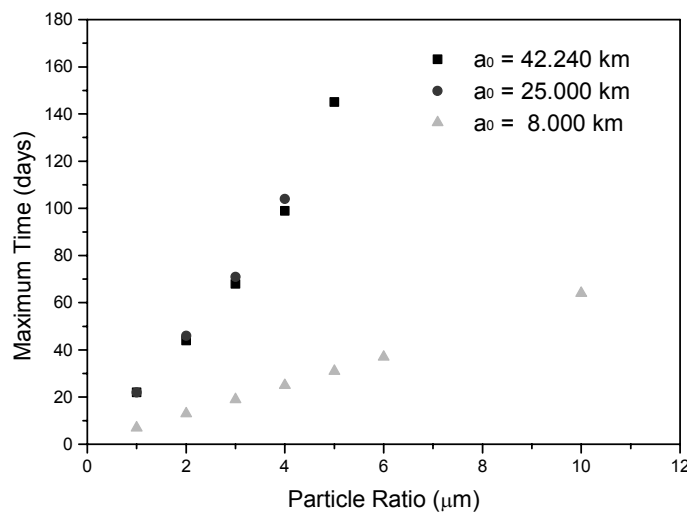

Figure 9. Time interval for the particle to enter in the region where the predominant disturbing force is the atmospheric drag versus particles in high, intermediate and low orbits around the Earth. The time for the particle to enter in this region depends on the size and of the particle orbital region.

REFERENCES

Burns, J.A.; Lamy, P.L.; Soter, S., 1979. "Radiation Forces on Small Particles in the Solar System". Icarus, **40**, pp. 1- 48.

Foryta, D.W.; Sicardy, B., 1996. " The Dynamics of the Neptunian Adams Ring's Arcs". Icarus, **123**, pp. 129-167.

Grün, E.; Zook, H.A.; Fechtig, H.; Giese, H., 1985. "Collisional Balance of the Meteoritic Complex". Icarus, **62**, pp. 244-272.

Hamilton, D.P.; Krivov, A.V., 1996. "Circumplanetary Dust Dynamics: Effects of Solar Gravity, Radiation Pressure, Planetary Oblateness and Electromagnetic". Icarus, Vol. **123**, pp. 503-523.

Hamilton, D.P.; Burns, J.A., 1992. "Orbital Stability Zones about Asteroids − II. The Destabilizing Effects of Eccentric Orbits and of Solar Radiation". Icarus, **96**, pp. 43-64.

Ishimoto, H., 1996. " Formation of Phobos/Deimos Dust Rings". Icarus, **122**, pp. 153-165.

Juhász, A.; Horányi, M., 1995. "*Dust Torus Aronnd* Mars". .Journal of Geophysical Research, **100**, pp. 3277-3284 (E2).

Krivov, A.; Kimura, H.; Mann, I., 1998. "Dinâmics of Dust Near the Sun". Icarus, Vol.**134**, pp. 311-327.

Krivov, A.V.; Sokolov, L.L.; Dikarev, V.V., 1996. "*Dynamics of Mars-Orbiting Dust: Effects of Light Pressure and Planetary Oblateness*". Celestial Mechanics and Dynamical Astronomy, **63**, pp. 3 13-339.

Liou, J-C.; Zook, A.H., 1997. "Evolution fo Iterplanetary Dust Particles in Mean Motion Resonances with Planets". Icarus, Vol. **128**, pp. 354-367.

Mignard, F., 1982. "Radiation Pressure and Dust Particle Dynamics". Icarus , Vol. **49**, pp. 347-366.